Athermal Simulation of Plastic Deformation in Amorphous Solids at Constant Pressure

MARCEL UTZ,[1,2] QING PENG,[2] MAGESH NANDAGOPAL[1]

[1]Institute of Materials Science, University of Connecticut, Storrs, Connecticut 06269

[2]Department of Physics, University of Connecticut, Storrs, Connecticut 06269

Received 21 October 2003; received 14 January 2004; accepted 27 January 2004
DOI: 10.1002/polb.20092
Published online in Wiley InterScience (www.interscience.wiley.com).

ABSTRACT: An algorithm is introduced for the molecular simulation of constant-pressure plastic deformation in amorphous solids at zero temperature. This allows to directly study the volume changes associated with plastic deformation (dilatancy) in glassy solids. In particular, the dilatancy of polymer glasses is an important aspect of their mechanical behavior. The new method is closely related to Berendsen's barostat, which is widely used for molecular dynamics simulations at constant pressure. The new algorithm is applied to plane strain compression of a binary Lennard-Jones glass. Conditions of constant volume lead to an increase of pressure with strain, and to a concommitant increase in shear stress. At constant (zero) pressure, by contrast, the shear stress remains constant up to the largest strains investigated ($\varepsilon = 1$), while the system density decreases linearly with strain. The linearity of this decrease suggests that each elementary shear relaxation event brings about an increase in volume which is proportional to the amount of shear. In contrast to the stress–strain behavior, the strain-induced structural relaxation, as measured by the self-part of the intermediate structure factor, was found to be the same in both cases. This suggests that the energy barriers that must be overcome for their nucleation continually grow in the case of constant-volume deformation, but remain the same if the deformation is carried out at constant pressure. © 2004 Wiley Periodicals, Inc. J Polym Sci Part B: Polym Phys 42: 2057–2065, 2004

INTRODUCTION

The glassy state of matter continues to present many scientific challenges, despite a large amount of research devoted to it over the past century.[1] In particular, the response of amorphous solids to large amounts of deformation is not yet completely understood.[2] It is meanwhile widely accepted that plastic deformation of glasses proceeds via the nucleation of stress-induced relaxation events.[2] This has been demonstrated by computer simulations of the deformation process in a number of different systems.[3–9] In addition, the stress–strain behavior of glassy solids depends strongly on their thermal history, suggesting an intimate coupling between the slow relaxation processes that cause physical aging, and the strain-induced relaxation during plastic deformation.[10] The precise nature of these relaxation processes seems to depend strongly on the material. Although in atomic glasses, computer simulations show a high degree of localization of the relaxation events to about one nearest neighbor shell, no such localization has to date been observed in simulations of the deformation of

Correspondence to: M. Utz (E-mail: marcel.utz@uconn.edu; URL:http://giotto.ims.uconn.edu/~mutz)

Journal of Polymer Science: Part B: Polymer Physics, Vol. 42, 2057–2065 (2004)

glassy polymers. Indeed, there is experimental evidence that the strain-induced relaxation in polymers is much more diffuse, and that the relevant size scale is set by the entanglement density of the polymer network.[11,12]

The nature of the discrete relaxation events during plastic deformation of polymer glasses is currently an unsolved problem of polymer physics. An aspect of particular importance concerns the volume change associated with the plastic relaxation events. Volume changes associated with shear deformation are commonly referred to as dilatancy. Experimental evidence suggests that there is a link between the availability of free volume in the amorphous polymer packing and the resistance to plastic yielding.[13] The shear activation volume, a parameter that describes the dependence of the yield stress on the applied strain rate,[2,14] is also known empirically to depend weakly on the isotropic component of the stress tensor in glassy polymers,[15,16] in the sense that hydrostatic pressure makes plastic deformation harder.

Apart from the fundamental interest in dilatancy as an aspect of the nature of plastic relaxation processes, volume changes that accompany shear deformation directly influence material behavior. Examples include the formation of shear bands in fiber composites, which has been shown to depend on the dilatancy of the matrix,[17] and the initiation of microbuckling defects in fiber composites under multiaxial loading.[18]

Direct volumetric observation of the density changes associated with plastic deformation of polymer glasses is difficult, due to the interference of the elastic Poisson effect. Experimental results on glassy polymers have mostly shown a positive dilatancy (volume increase with shear deformation),[19] although the literature is not unanimous on this point (ref. 20, and references cited therein). Computer simulations could be very helpful to clarify this situation.

However, most computer simulations of plastic flow in glassy solids have been performed at constant volume. In general, this leads to an increase in system pressure with shear strain due to the dilatancy:[2] the strain-activated localized relaxation events not only bring about shear, but also an increase in volume. If the total system volume is constrained during the simulation, a concommitant increase in system pressure results.[7,21] Although a positive correlation between strain and system pressure has been observed in most simulations, this seems to depend strongly on the material studied. Indeed, Hutnik et al. have observed a *negative* dilatancy in the plastic deformation of polycarbonate.[6] In contrast to these simulations, experimental studies of plasticity are usually conducted not at constant volume, but at constant pressure. Because in most amorphous solids the elementary processes of plastic relaxation are known to be dilatant, it is possible *a priori* that the kinematics of relaxation are affected by the constraint of constant volume.

In the present contribution, we introduce an algorithm that allows to perform athermal deformation simulations under conserved pressure, rather than at constant volume, and we apply it to study the plane strain response of a binary Lennard-Jones glass. This allows to study the strain-induced relaxation at $P = 0$, that is, under a purely deviatoric stress state. As will be shown in the following, constant-volume simulations lead to a increase in shear stress at high strains due to the pressure buildup. By contrast, at constant pressure, no such increase is observed, while the density of the system decreases linearly with strain. In contrast to the stress–strain response, the kinematics of the relaxation processes, as measured by the decay of the intermediate structure factor, seem to be the same in both cases.

This new algorithm allows the direct simulation of dilatant shear deformation in glassy materials, including the concomitant volume change. The purpose of the present article is to introduce the method, and to demonstrate its principle. In a future contribution, we will report its application to simulate the plastic response of polymer glasses.

Recently, it has been realized from computer simulations that the deformation-induced relaxation processes in atomic glasses lead to an exponential decay of the self part of the intermediate structure factor, similar to thermal relaxtion of the liquid at temperatures sufficiently above the glass transition. This has been verified both in systems under continous simple shear flow[21–25] and in transient deformation simulations.[26]

In a recent publication,[27] we have investigated the interplay between thermal and deformation-induced relaxation in a binary Lennard-Jones glass. It was found that thermal and deformation-induced relaxation processes involve similar particle kinematics, and that they superimpose linearly when both occur at the same time. Such simulations, even though they are carried out using a model atomic glass, can give valuable insight on the microscopic nature of phenomena

that are observed in a much wider range of glassy materials. For instance, simulations of Lennard-Jones glass have shown that physical aging of the glass leads to the development of a maximum in the stress–strain curve at the yield point, and that the effects of aging are erased by moderate amounts of plastic deformation.[21] This corresponds to a well-known behavior of polymer glasses,[10] indicating that the phenomenon is general, and can be seen in all glasses if the time scales allow its observation.

Simulation Method

Plastic deformation can be simulated in the absence of thermal relaxation (i.e., at $T = 0$) in the following way: in a first step, the extents of the periodic simulation cell are changed by a small amount corresponding to the desired strain increment. In a second step, the potential energy of the system is minimized with respect to the fractional coordinates of all particles using a conjugate-gradient method. This procedure ensures that the system is maintained at the bottom of a potential energy well. If the strain increments are chosen sufficiently small, the system's trajectory will follow the lowest potential energy path compatible with the prescribed strain. This method has been applied successfully to a variety of different systems in the past.[3,6–8,21,28,29]

Deformation at constant volume is easily implemented in the above method by using a volume-conserving strain increment. In the present contribution, we introduce an extension of this method that allows for simulations to approximate conditions of conserved pressure instead. The algorithm is closely related to the Berendsen barostat,[28,29] which is widely used to keep pressure constant in molecular dynamics simulations.[30]

After each deformation step, the stress tensor T is calculated from the generalized internal virial tensor

$$\Xi_{nm} = \sum_{i<j} r_{ij,n} f_{ij,m}, \quad \text{where } n, m = x, y, z, \tag{1}$$

where $r_{ij,n}$ and $f_{ij,n}$ are the components of the displacement and force vectors between particles i and j, respectively. The components of the stress tensor are given by

$$T_{nm} = -\frac{\Xi_{nm}}{V}, \tag{2}$$

where V is the system volume. Note that at finite temperature, (2) would contain a kinetic energy (ideal gas) term, also. The instantaneous system pressure is then given by the trace of the stress tensor

$$P = -\frac{1}{3} TrT. \tag{3}$$

The constant pressure simulation method introduced here aims at an evolution of the system pressure P with deformation ε that obeys the differential equation

$$\frac{dP}{d\varepsilon} = -\frac{P - P_0}{\varepsilon_P}, \tag{4}$$

where P_0 is a given target pressure, and ε_P is the pressure relaxation strain, which is analogous to the pressure relaxation time introduced by Berendsen et al.[28]

In practice, the choice of ε_P is quite straightforward. On the one hand, a small value of ε_P is desirable, to ensure an accurately isobaric simulation. On the other hand, values of ε_P that are small compared to the deformation step size $\delta\varepsilon$ lead to numerical instabilities. Thus, reasonable values of ε_P must lie in the neighborhood of 1. . .5 $\delta\varepsilon$.

The rate of change in the pressure can be converted into a rate of change of the system volume by using the isothermal bulk modulus K:

$$dP = -K\frac{dV}{V}. \tag{5}$$

We obtain

$$\frac{dV}{V} = (P - P_0)\frac{d\varepsilon}{K\varepsilon_P}. \tag{6}$$

After each deformation/minimization step, the volume of the system is therefore adjusted by a factor e^{μ}, with

$$\mu = (P - P_0)\delta\varepsilon/(K\varepsilon_P). \tag{7}$$

Such an adjustment is easily achieved by altering the extents of the simulation box. Even though the bulk modulus K may not be precisely known for a given system, an estimated value can be used. Deviations from the true bulk modulus will

not alter qualitatively the system's trajectory; only the effective pressure relaxation strain ε_P will be slightly off the desired value.

For the present study, we have used a binary Lennard-Jones fluid that closely resembles the model introduced by Stillinger and Weber[31] for $Ni_{80}P_{20}$. The thermal dynamics of this system[32–35] as well as its behavior under shear[21,22,23,24,26] have been studied in great detail. The model used here consisted of 3200 type A and 800 type B atoms in an orthorhombic simulation box subject to periodic continuation conditions. The total potential energy was given by the sum of the pair contributions

$$E_{ij} = 4\varepsilon_{ij}[(\sigma_{ij}/r_{ij})^{12} - (\sigma_{ij}/r_{ij})^{6}] + c_{ij}r_{ij}^2 + d_{ij} \qquad (8)$$

for $r_{ij} < r_c$, where r_{ij} is the distance between atoms i and j, and ε_{ij} and σ_{ij} are the energy and length parameters, respectively. The constants c_{ij} and d_{ij} are introduced to render E_{ij} continuously differentiable at the cutoff radius r_c. The values of $\varepsilon_{AA} = 1.0$, $\varepsilon_{AB} = 1.5$ and $\varepsilon_{BB} = 0.5$, and $\sigma_{AA} = 1.0$, $\sigma_{AB} = 0.8$ and $\sigma_{BB} = 0.88$ were used. The masses of the particles of type A and type B were $m_A = 1.0$ and $m_B = 0.53$, respectively. The length of the simulation box was 15. A cutoff radius $r_c = 2.5$ was used in all the cases. All quantities in this contribution are expressed in terms of reduced units, i.e., length in units of σ_{AA}, energy in units of ε_{AA}, and stress in units of $\varepsilon_{AA}/\sigma_{AA}^3$

Deformation simulations departed from a glassy initial configuration, which had been obtained by equilibrating a system of 4000 atoms by molecular dynamics at a high temperature, and subsequent energy minimization. A plane strain deformation mode was used with a strain increment[36]

$$\delta\varepsilon = \begin{bmatrix} \delta\varepsilon_{xx} & 0 & 0 \\ 0 & 0 & 0 \\ 0 & 0 & \delta\varepsilon_{zz} \end{bmatrix}, \qquad (9)$$

and a constant deformation step $\delta\varepsilon_{zz} = -0.00125$. This corresponds to a plane strain compression. Under conditions of conserved sample volume, or for an ideally incompressible material, $\varepsilon_{xx} = -\varepsilon_{zz}$. In general, the change in volume per deformation step is given by

$$\mu = \ln\frac{V + \delta V}{V} = \delta\varepsilon_{xx} + \delta\varepsilon_{zz}. \qquad (10)$$

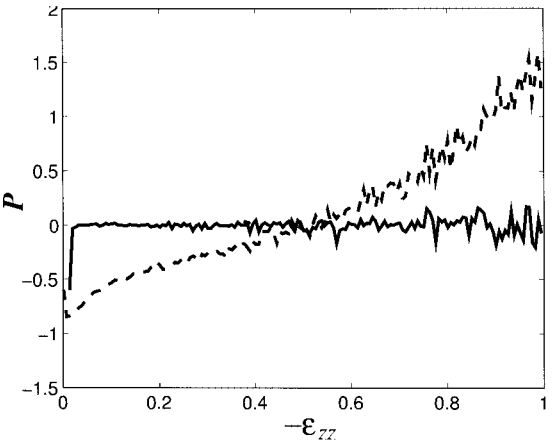

Figure 1. System pressure P (in units of $\varepsilon_{AA}/\sigma_{AA}^3$) as a function of deformation for $\varepsilon_P = \infty$ (dashed line) and $\varepsilon_P = 0.0033$ (solid line). The data shown represents the average of 20 independent simulation runs.

To ensure conditions of constant pressure, $\delta\varepsilon_{xx}$ was calculated prior to each deformation step according to (7):

$$\delta\varepsilon_{xx} = \delta\varepsilon_{zz}\left(\frac{P - P_0}{K\varepsilon_P} - 1\right). \qquad (11)$$

RESULTS AND DISCUSSION

Pressure Conservation

To carry out constant pressure simulations, a reasonably accurate estimate for the bulk modulus K is needed. In the present case, this was obtained from the elastic shear modulus observed in constant volume simulations, assuming a Poisson's ratio of 0.3. This yields a value of $K \approx 49.8$, in units of $\varepsilon_{AA}/\sigma_{AA}^3$. This is admittedly a crude way of estimating K, and a dedicated simulation using an isotropic deformation would almost certainly have yielded a more reliable value. However, the precise value of K is of little concern, because it is the product $K\varepsilon_P$ that actually enters the simulation.

The system pressure and density as a function of deformation are shown in Figures 1 and 2, respectively, for values of $\varepsilon_P = \infty$ (corresponding to constant volume, dashed line), and $\varepsilon_P = 0.0033$ (approximating constant pressure conditions, solid line). Each of the two data sets shown represents the average of 20 independent simulation runs, departing from different starting configurations.

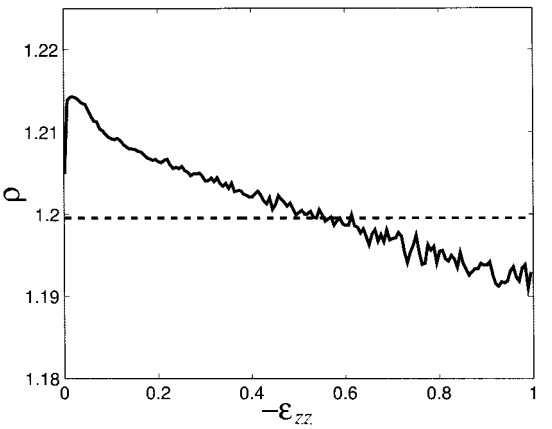

Figure 2. Number density of particles ρ (in units of $1/\sigma_{AA}^2$) as a function of deformation for $\varepsilon_P = \infty$ (dashed line) and $\varepsilon_P = 0.05$ (solid line). The data shown represents the average of 20 independent simulation runs.

In both cases, the system starts out at a state of slight isotropic tension, with a pressure of $P = -0.6$. This is due to the chosen initial density, which leads to zero pressure in molecular dynamics simulations at $T = 1.0$. After energy minimization, in the absence of thermal motion, the observed tension results.

It is clearly obvious from Figure 1 that at constant volume ($\varepsilon_P = \infty$), the system pressure increases systematically with deformation after a brief stage of pressure reduction associated with the elastic response. This initial response is due to the fact that the Poisson ratio for the material under study is close to $\nu = 0.3$, so that elastic plane strain compression is accompanied by a slight reduction in volume. Because the dashed curve in Figure 1 has been obtained at *constant* volume, a decrease in pressure results. After a few precent of strain, the pressure increases monotonously with the deformation. This effect has been observed by several authors working on a number of different systems.[7,21] For a finite value of ε_P, however, a different behavior results. The initially negative pressure rapidly approaches the target value of $P_0 = 0$, which is reached at about 1% strain. Correspondingly, the structure densifies (Fig. 2) from the initial $\rho = 1.200$ to $\rho = 1.215$.

After this initial phase, the system density continually falls with increasing deformation. After the yield point, which occurs at about 8% deformation in this system,[21,26] there is a linear dependence of the density on strain, with a slope of $(d\mathrm{P})/(d\varepsilon_{zz}) = 0.0175 \pm 0.0005$. The pressure remains constant, with small fluctuations about the target value of $P_0 = 0$. These results demonstrate that the method described above indeed does keep the pressure constant, and they illustrate the dilatant nature of the plastic deformation process.

Of course, the results are somewhat sensitive to the selection of ε_P. We have found that similar results can be obtained with a wide range of choices for the relaxtion strain ε_P. Figure 3 shows the system pressures for a range of different values of ε_P. For $\varepsilon_P > 1$, the barostat is not sufficiently effective to compensate for the dilatancy, and a systematic drift in the system pressure results (first column in Fig. 3). On the other hand, $\varepsilon_P < 0.002$ results in increasing magnitude of the density fluctuations with strain, and at $\varepsilon_P = 0.00125$, the computation becomes numerically unstable at deformations greater than about 0.6. This leaves a window for ε_P of $0.002 < \varepsilon_P < 0.05$ that offers good pressure conservation without excessive fluctuations. We have chosen a value of $\varepsilon_P = 0.0033$ as a working compromise for the purposes of the present study.

Stress–Strain Behavior

Running the deformation under conditions of conserved system pressure was found to have a profound effect to the evolution of the shear stress with deformation, in particular, at large deformations. Figure 4 shows the von Mises equivalent shear stress as a function of ε_{zz} for both constant volume ($\varepsilon_P = \infty$) and constant pressure ($\varepsilon_P = 0.0033$). The von Mises equivalent stress, essentially the second invariant of the stress tensor, is a positive measure of the amount of shear stress present, and is defined as

$$\sigma_{eq} = \sqrt{\frac{3}{2}\, tr(\mathbf{t}_d \cdot \mathbf{t}_d)}, \tag{12}$$

where $\mathbf{t}_d$ is the deviatoric part of the stress tensor

$$\mathbf{t}_d = \mathbf{t} + P\mathbf{I}, \tag{13}$$

with the identity tensor **I.**

At small strains, the von Mises stress behaves similar for both constant volume and constant pressure: an elastic linear increase is followed by a plastic regime, where σ_{eq} is more or less independent of strain. The yield stress, as measured by the plateau value in σ_{eq} seems to be slightly lower in the case of constant volume. Marked differences between the two cases become appar-

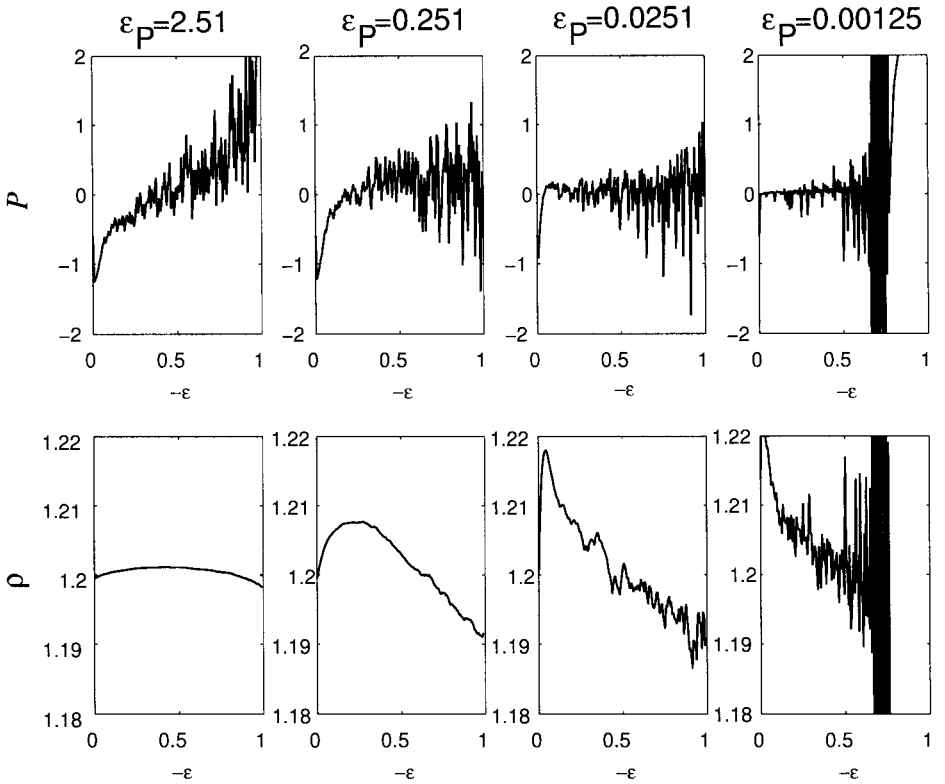

Figure 3. Effect of different choices of the relaxation strain ε_P on the evolution of pressure (top row) and density (bottom row) over the course of a plane–strain deformation simulation from $\varepsilon_{zz} = 0$ to $\varepsilon_{zz} = 1$. For each value of ε_P, results from a single simulation run are shown.

ent at high deformations, above about $|\varepsilon_{zz}| = 0.3$. Whereas at constant pressure, the von Mises stress continues to fluctuate slightly around the same plateau value, it raises increasingly rapidly in the case of constant volume.

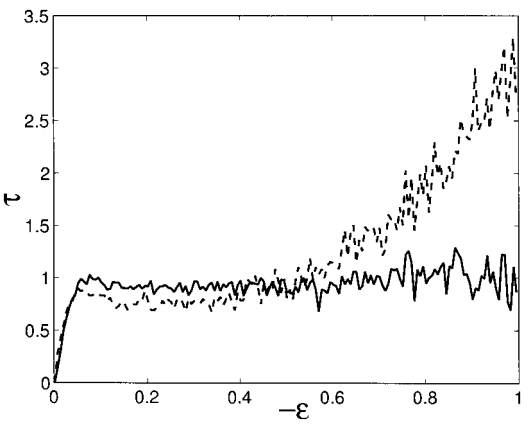

Figure 4. Von Mises equivalent shear stress τ as a function of strain ε_{zz} for relaxation strain $\varepsilon_P = \infty$ (dashed line) and $\varepsilon_P = 0.0033$ (solid line). Each data set shown is the average of 20 independent simulation runs.

This increase can easily be understood by the buildup of system pressure, which progressively hinders dilatant shear relaxation events. As a result, only shear relaxation events with a small amount of local increase in volume are nucleated. This leads to the observed increase in resistance to shear.

Under constant pressure conditions, no such effect is observed. The von Mises equivalent stress remains at the same value up to the maximum deformation probed in the present simulations. Figure 4 shows a small increase in the magnitude of the stress fluctuations at high strains. The fluctuations are due to the finite size of the simulation cell. Because the cell goes from a cubic shape at $\varepsilon_{zz} = 0$ to an elongated shape at $\varepsilon_{zz} = -1$, its thickness in the z direction continually decreases during the course of the simulation. This leads to less efficient averaging of the normal stress component t_{zz} in the later stages of the deformation. Because t_{zz} provides a dominant

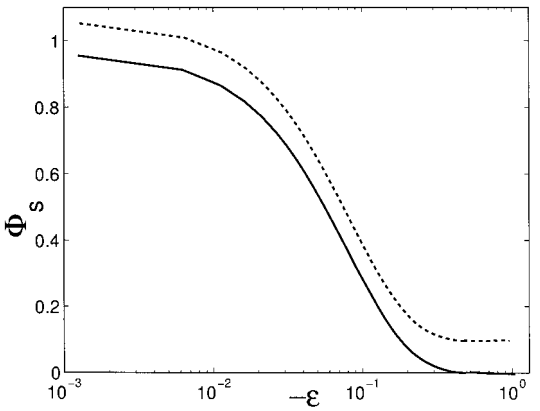

Figure 5. Self part of the isotropically averaged intermediate structure factor $\Phi_s(k, \varepsilon_{zz})$ as a function of strain ε_{zz} for constant volume ($\varepsilon_P = \infty$, dashed line), and constant pressure ($\varepsilon_P = 0.0033$, solid line). The dashed curve has been displaced vertically by 0.1; otherwise, the two curves would coincide to within the line width. $k = 7.251$ in both cases; corresponding to the location of the maximum in the static structure factor.

contribution to both P and σ_{eq}, the fluctuations in these values increase over the course of the simulation.

Strain-Induced Structural Relaxation

The structural relaxation of amorphous solids can be monitored conveniently by the decay of the self part of the intermediate structure factor,

$$\Phi_s(\mathbf{k}, t) \propto \int G_s(\mathbf{r}, t) e^{-i\mathbf{k}\mathbf{r}} d\mathbf{r}, \qquad (14)$$

where the van Hove correlation function $G_s(\mathbf{r},t)d\mathbf{r}$ is proportional to the probability of observing a particle within $d\mathbf{r}$ of $\mathbf{r}$ at time t, given that it was located at the origin at time 0,[37] $\Phi_s(\mathbf{k}, t)$ is normalized such that $\Phi_s(\mathbf{k}, 0) \equiv 1$.

In the present case, where plastic deformation is simulated under exclusion of thermal relaxation, time has no meaning, and must be replaced by the strain that continually increases during the simulated trajectory. Therefore, in the present context the relevant correlation functions are $G(\mathbf{r}, \varepsilon_{zz})$ and $\Phi_s(\mathbf{k}, \varepsilon_{zz})$.[26]

The isotropically averaged relaxation functions $\Phi_s(k, \varepsilon_{zz})$ are shown in Figure 5 for $k = |\mathbf{k}| = 7.251$ (this value corresponds to the position of the maximum of the static structure factor). In both cases, the contribution of the affine deformation to the decay of Φ_s, which is purely caused by the shape change of the simulation box and not the rearrangement of the atoms inside it, has been removed according to a procedure described in detail in ref. 26.

The curves for constant pressure and constant volume are indistinguishable; they had to be displaced from one another in Figure 5 to avoid coincidence. This result contrasts sharply with the pronounced difference in the stress–strain behavior of the two cases. It suggests that the kinematics of the relaxation events nucleated by plastic deformation in the present binary Lennard-Jones system are *the same* under conditions of constant pressure and constant volume.

This seems surprising, given the marked differences in the von Mises equivalent stress between the two cases. *A priori,* it seems quite possible that the intermediate structure factor is not a sensitive measure of the change in kinematics. To rule out this possibility, the structure of the simulation systems were carefully investigated at different levels of deformation. No differences apart from the change in density in the case of conserved pressure could be identified. In particular, the pair-correlation functions $g_{AA}(r)$, $g_{BB}(r)$, and $g_{AB}(r)$, measuring the distribution of $A - A$, $B - B$, and $A - B$ particle pairs, respectively, have been investigated as a function of deformation. The pair correlation functions were not affected by the deformation, and no differences between the cases of constant volume and constant pressure could be identified. As an example, $g_{BB}(r)$ is shown in Figure 6 for both constant pressure (solid lines) and constant volume (dashed lines), at $-\varepsilon_{zz} = 0$, 0.2, 0.5, and 0.9, respectively. g_{BB} has been shown to provide a sensitive measure of the state of the system, because contacts between B particles are energetically disfavored by the force field.[21] The fact that $g_{BB}(r)$ does not differ between systems deformed at constant pressure and constant volume therefore suggests that they are indeed structurally identical, up to a small difference in density.

The evolution of the potential energy landscape of atomic glasses upon changes in density has been investigated in detail by Malandro and Lacks.[38] They found that reducing the density leads first to a lowering in the energy barrier between adjacent minima ("inherent structures"[39,40]) and then to their complete disappearance. Malandro and Lacks reported that a 3% decrease in volume leads to the loss of about one quarter of the possible inherent structures.[38]

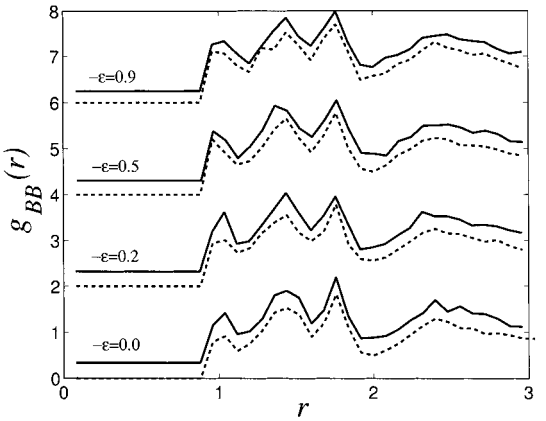

Figure 6. Pair correlation functions $g_{BB}(r)$ for different degrees of deformation (as indicated in the figure). Solid lines: constant pressure ($\varepsilon_P = 0.0033$); Dashed line: constant volume ($\varepsilon_P = \infty$). The curves have been vertically displaced to avoid coincidence.

Their study used a single-component atomic glass; however, a similar behavior of the binary Lennard-Jones fluid studied here must be expected. In the present case, shear deformation at constant volume seems to lead to an *increase* of the height of energy barriers between adjacent minima, as manifested by the increase in the von Mises equivalent stress. Under conditions of constant pressure, this increase is apparently perfectly compensated by the decrease in density, leading to a constant von Mises stress.

CONCLUSIONS

In summary, an algorithm similar to Berendsen's barostat has been introduced for the simulation of plastic deformation of glassy solids at constant pressure, and it has been successfully applied to the plane strain compression of a binary Lennard-Jones fluid. The dilatant nature of the elementary plastic relaxation processes was clearly demonstrated by a linear decrease of density with strain with a slope of $(d\mathrm{P})/(d\varepsilon_{zz}) = 0.0175 \pm 0.0005$.

Although no difference in the strain-induced structural relaxation of the system could be identified between the cases of constant pressure and constant volume, the response of the von Mises equivalent shear stress to deformation is strongly affected. Conditions of constant volume lead to a build-up of system pressure with deformation, which, in turn, leads to an increase of resistance to further deformation, that is, an increase in the von Mises equivalent stress. In the case of constant pressure, no such effect is observed, and the von Mises equivalent stress remains at the level of the yield point over the entire range of deformation.

The results presented in this contribution give rise to a number of questions. On the one hand, it is entirely unclear what determines the specific value of the observed dilatancy. Simulations on different molecular and atomic glasses are currently underway in our laboratory, to obtain information on the variability of the dilatancy in different systems. On the other hand, the fact that no change in the pair correlation functions was found as a function of deformation in the case of constant volume is intriguing. This means that glasses with the same pair correlation functions can exhibit widely different pressures. However, at zero temperature, the arrangement of the atoms is the *only* factor that influences the system pressure. The systems therefore must be structurally different before and after shear deformation at constant volume. We are currently exploring higher order correlation functions as a means to quantify these subtle differences.

We are indebted to Greg McKenna for helpful discussions. This work was supported by the National Science Foundation by an Early Career Development Award to M.U. (DMR-0094290), and by a Junior Faculty Award to M.U. from Petroleum Research Fund, administered by the American Chemical Society (PRF-36246-G7).

REFERENCES AND NOTES

1. Angell, C. A. Science 1995, 267, 1924.
2. Argon, A. S. Materials Science and Technology; VCH: Weinheim, 1993, Chap 10, pp 462–508.
3. Srolovitz, D.; Vitek, V.; Egami, T. Acta Met 1983, 31, 335.
4. Maeda, K.; Takeuchi, S. J Phys 1982, F 12, 2767.
5. Deng, D.; Argon, A. S.; Yip, S. Philos Trans R Soc Lond A 1989, 329, 613.
6. Hutnik, M.; Argon, A. S.; Suter, U. W. Macromolecules 1993, 26, 1097.
7. Mott, P. H.; Argon, A. S.; Suter, U. W. Philos Mag A 1993, 67, 931.
8. Malandro, D. L.; Lacks, D. J. J Chem Phys 1999, 110, 4593.
9. Utz, M.; Debenedetti, P. G.; Stillinger, F. H. Phys Rev Lett 2000, 84, 1471.
10. Hasan, O. A.; Boyce, M. C. Polymer 1993, 34, 5085.
11. Henkee, C. S.; Kramer, E. J. J Polym Sci: Polym Phys 1984, 22, 721.

12. Ho, J.; Govaert, L.; Utz, M. Macromolecules 2003, 36, 7398.
13. Hasan, O. A.; Boyce, M. C.; Li, X. S.; Berko, S. J Polym Sci: Polym Phys 1993, 31, 185.
14. Argon, A. S.; Bulatov, V. V.; Mott, P. H.; Suter, U. W. J Rheol 1995, 39, 377.
15. Ward, I. M. Mechanical Properties of Solid Polymers; Wiley-Interscience: London, 1971.
16. Tervoort, T. A. PhD Thesis, Technical University Eindhoven, 1996.
17. Vogler, T.; Hsu, S.-Y.; Kyriakides, S. Int J Solids Struct 2001, 38, 2653.
18. Shu, J.; Fleck, N. Proc R Soc Lond Ser. A 1997, 453, 2063.
19. Waldron, W. K.; McKenna, G. B. J Rheol 1995, 39, 471.
20. Struik, L. C. E. Polymer 1997, 38, 4053.
21. Barrat, J.-L.; Berthier, L. Phys Rev E 2001, 63, 012503/1.
22. Berthier, L.; Barrat, J.-L.; Kurchan, J. Phys Rev E 2000, 61, 5464.
23. Berthier, L.; Barrat, J.-L. J Chem Phys 2002, 116, 6228.
24. Berthier, L.; Barrat, J.-L. Phys Rev Lett 2002, 89, 095702/1.
25. Ono, I. K.; O'Hern, C. S.; Durian, D. J.; Langer, S. A.; Liu, A. J.; Nagel, S. R. Phys Rev Lett 2002, 89, 095703/1.
26. Nandagopal, M.; Utz, M. J Chem Phys 2003, 118, 8373.
27. Lacks, D. J. Phys Rev Lett 1998, 80, 5385.
28. Berendsen, H. J. C.; Postma, J. P. M.; van Gunsteren, W. F.; DiNola, A.; Haak, J. R. J Chem Phy 1984, 81, 3684.
29. van Gunsteren, W.; Berendsen, H. Angew Chem Int Ed Engl 1990, 29, 992.
30. Allen, M. P.; Tildesley, D. J. Computer Simulation of Liquids; Clarendon Press; Oxford, 1987.
31. Weber, T. A.; Stillinger, F. H. Phys Rev B 1985, 32, 5402.
32. Kob, W.; Andersen, H. C. Phys Rev Lett 1994, 73, 1376.
33. Kob, W.; Andersen, H. C. Phys Rev E 1995, 51, 4626.
34. Kob, W.; Andersen, H. C. Phys Rev E 1995, 52, 4134.
35. Sastry, S.; Debenedetti, P. G.; Stillinger, F. H. Nature 1998, 393, 554.
36. The strain is defined as $\varepsilon = \ln(a_t/a_0)$ where a_t is the cell demension at time t, and a_0 is the reference dimension of the simulation cell.
37. Debenedetti, P. G. Metastable Liquids: Concepts and Principles; Princeton University Press: Princeton J, 1996.
38. Malandro, D. L.; Lacks, D. J. J Chem Phys 1997, 107, 5804.
39. Stillinger, F. H.; Weber, T. A. Phys Rev A 1985, 28, 2408.
40. Stillinger, F. H. Science 1995, 267, 1935.